

Interactive report

Response dynamics of entorhinal cortex in awake, anesthetized, and bulbotomized rats[☆]

Kurt F. Ahrens^{a,*}, Walter J. Freeman^b

^aDepartment of Physics, University of California, San Diego, 7108 Urey Hall, m.c. 0319, 9500 Gilman Dr., La Jolla, CA 92093-0319, USA

^bDepartment of Molecular and Cell Biology, University of California, Berkeley, Berkeley, CA, USA

Accepted 4 June 2001

Abstract

The generation of oscillatory activity may be crucial to brain function. The coordination of individual neurons into rhythmic and coherently active populations is thought to result from interactions between excitatory and inhibitory cells mediated by local feedback connections. By using extracellular recording wires and silicon microprobes to measure electrically evoked damped oscillatory responses at the level of neural populations in the entorhinal cortex, and by using current-source density analysis to determine the spatial pattern of evoked responses, we show that the propagation of activity through the cortical circuit and consequent oscillations in the local field potential are dependent upon background neural activity. Pharmacological manipulations as well as surgical disconnection of the olfactory bulb serve to quell the background excitatory input incident to entorhinal cortex, resulting in evoked responses without characteristic oscillations and showing no signs of polysynaptic feedback. Electrical stimulation at 200 Hz applied to the lateral olfactory tract provides a substitute for the normal background activity emanating from the bulb and enables the generation of oscillatory responses once again. We conclude that a non-zero background level of activity is necessary and sufficient to sustain normal oscillatory responses and polysynaptic transmission through the entorhinal cortex. © 2001 Elsevier Science B.V. All rights reserved.

Theme: Other systems of the CNS

Topic: Limbic system and hypothalamus

Keywords: Oscillation; Nonlinear dynamics; Olfactory system; Local field potential; Current source density

1. Introduction

Rhythmic oscillations and coherent neuronal activity are thought to be important aspects of brain function because of their presence within and across many brain regions and their correlation with behavioral states [3,7,31]. The role played by coordinated and rhythmic activity is not fully understood, but it is clear that simultaneous inputs provide more effective stimulation to a postsynaptic neuron than random firing. Correlated inputs may result in changes in synaptic efficacy as well, through LTP or LTD [25]. The entorhinal cortex (EC) exhibits several distinct rhythms

characteristic of mammals, notably the θ (8–12 Hz) [1], β (12–30 Hz) [5], and γ (30–80 Hz) [8,9].

Proposed mechanisms for rhythmic neuronal activity include rhythmic driving by another structure [2,11], intracellular oscillations (resulting from feedback interactions between hyperpolarizing and depolarizing currents) [15,30], and feedback interactions between intracortical neuronal populations [17,36]. None of these are mutually exclusive, and finding evidence for all may be an indication of the importance of cortical oscillations from an evolutionary standpoint.

The presence of interconnected networks of excitatory and inhibitory cells indicates the possibility of both positive and negative feedback, each of which might contribute to the generation of oscillations. To investigate the interactions of neural populations in the EC, we characterized its response to electrical stimulation of the lateral olfactory tract (LOT) in awake and anesthetized

[☆]Published on the World Wide Web on 19 June 2001.

*Corresponding author. Tel.: +1-858-534-3562; fax: +1-858-534-7697.

E-mail address: kurt@ucsd.edu (K.F. Ahrens).

animals. Normal evoked responses are damped oscillations in the β frequency range; however, conditions that reduce the tonic excitatory drive to the EC eliminate the oscillatory component of the response. Loss of the activating drive leaves the neural elements refractory to stimulation (e.g. further from threshold), thereby preventing signal propagation through the putative feedback loops and resulting in ‘open loop’ responses. This effect is reversible with artificial tonic activation in the form of a high frequency pulse train delivered to the LOT.

2. Materials and methods

All experimental and surgical procedures used in these studies were approved by the Animal Care and Use Committee at the University of California, Berkeley. A total of 16 rats were used in chronic experiments, 12 in the acute bipolar recording experiments, 15 in the current-source density experiments, and 12 in the bulbotomy experiments.

Male and female rats of the Sprague–Dawley and Long–Evans strains were used in these experiments. Prior to surgery, the animals were sedated (ketamine (50 mg/kg), xylazine (5 mg/kg), and acepromazine (0.5 mg/kg), injected subcutaneously) and catheterized in the tail vein. Surgical anesthesia was thereafter maintained by intravenous injection of Nembutal (25 mg/kg for males, 12.5 mg/kg for females), with supplemental doses given when needed. Local anesthetic (Lidocaine, 2% solution) was applied to the site of incision to reduce noxious stimulation. Temperature was monitored and maintained at 37°C throughout surgery, and during recovery for chronically implanted animals.

During surgery, animals were held in a stereotaxic frame with earbars and an incisor bitebar. The head was held in the ‘flat skull’ position [33] for stereotaxic electrode placement. A single midline incision was made, extending from between the eyes to 2 mm posterior to the lambda point. Tissue was reflected from the skull dorsum and trephine holes were drilled to provide access for electrodes and for support screws. All breaches of the skull were bathed in artificial cerebrospinal fluid. Small (00-80) stainless steel screws were inserted at two or more locations to provide a rigid foundation for cementing electrodes in place; these screws were also used for animal ground connections. In chronic surgeries, the support screws were placed with one in each temporal bone, providing a base that remained stable for months, even in the face of thread deterioration. Electrode hole positions were determined according to stereotaxic coordinates [33].

Bipolar electrodes were used for recording and stimulation. They consisted of two strands of formvar coated, 100- μ m diameter stainless steel wire (California Wire, Grover Beach, CA) glued together, with a tip separation from 0.2 to 1.5 mm. Small separations were used for

stimulating electrodes, allowing either wire to be an effective stimulator, while wider separations were used for recordings, to span the cortical layers of interest. Electrical connectors (amphenol, female) were attached to the peripheral ends of the wires. The LOT stimulating electrode was positioned grossly according to stereotaxic coordinates (Table 1); the depth was then optimized by observing the evoked potential strength in the olfactory bulb (OB). In some experiments, an additional stimulating electrode was placed at a separate location along the LOT (referred to as LOT 2; Table 1). Once the stimulating electrodes were positioned, recording electrodes were placed. The polarity of the evoked potential measured on the longer wire would reverse once the signal generating cell layers had been crossed. Differential recording across the generator layers produced a strong signal, free of contamination from distant brain areas.

Wire electrodes were cemented in place with dental acrylic. To prevent wires from slipping through the cement, a small drop of Superglue was placed at the interface of wire and cement. Electrode connectors were inserted into a nine-pin round threaded socket. In chronic surgeries, the wires and socket were embedded in cement and the wound was closed with surgical staples.

Silicon probes (University of Michigan Center for Neural Communication Technology, Ann Arbor, MI) with 16 iridium recording sites (100 μ m²) in a linear array were used to record field potentials in the EC, in some acute experiments. Recording sites were 100 μ m apart; simultaneous recordings were made along a line perpendicular to the cortical surface, extending from the surface to a depth of 1.5 mm. Use of these probes necessitated opening the skull immediately superficial to the EC, anterior and ventral to the auditory canal. This exposure required removal of a portion of the mandible and the overlying muscle. Once the cortex was exposed, the silicon probe was positioned by visual inspection under a surgical microscope.

Surgical transection of the stalk of the OB was achieved

Table 1
Stereotaxic coordinates of electrode targets

Structure	Purpose	A–P (mm)	M–L (mm)	D–V (mm)
OB	Recording	9.0	1.5	3.5
EC	Recording	2.8 ^a	7.0	1.4
LOT 1	Stimulation	2.7	3.6	2.0
LOT 2	Stimulation	3.7	3.0	2.8

Recording electrodes were placed in the olfactory bulb (OB) and the entorhinal cortex (EC); stimulation electrodes were placed in the lateral olfactory tract (LOT) at two locations. The coordinates are defined in terms of the anterior–posterior axis (A–P), the medial–lateral axis (M–L), and the dorsal–ventral axis (D–V). Positive A–P values represent locations anterior of the point where the bregma suture crosses the midline (^aexcept in the case of the EC electrode, whose position was measured from the vertical interaural plane), positive M–L values represent locations on the animal’s left, and positive D–V values represent locations above the horizontal interaural plane.

by tissue aspiration in six animals and by bulbotomy in six animals. In either case, transection was performed at 5 mm anterior to the bregma reference point. In four animals, temporary OB inactivation was achieved by injection of 0.01 ml lidocaine (2% solution) at 5 mm anterior to bregma.

Rats were euthanized by lethal overdose of Nembutal (125 mg/kg) and wire electrode positions were marked with the Prussian blue reaction. The tissue was fixed by transcardial perfusion of buffered saline followed by a 4% paraformaldehyde solution. Electrode positions were verified by examination of thick sections under a surgical microscope in most cases; however, four brains were sectioned with a sliding microtome at 25- μ m thickness, mounted, and stained with cresyl violet. Silicon probe tracks were evident to microscopic examination in both thin and thick sections.

Data were collected and stimuli triggered by customized software running on a Macintosh computer with a 16-channel analog to digital converter and 64-channel multiplexer (National Instruments, Austin, TX). Electrical stimulation consisted of 10- μ s biphasic pulses (zero net current). Typically, 50 stimulus pulses were applied, with a mean interstimulus interval of 2 s. Averaged evoked potentials were calculated online. When two LOT stimulus sites were used, one (LOT 2) received a free running, i.e. continually present, 200-Hz train of pulses, while the other (LOT 1) received single pulses timelocked to data acquisition. Field potentials were filtered between 0.3 and 300 Hz for wire electrodes and 1–100 Hz for silicon probes, and digitized at 2000 samples per second for each channel. Offline data analysis was performed with Igor Pro software (WaveMetrics, Lake Oswego, OR).

Evoked potentials from deeply anesthetized rats were modeled as the sum of four exponentials, yielding an empirical transfer function for the open loop state, which was rewritten as a rational expression in frequency space by use of the Laplace transformation:

$$\sum_{i=1}^4 A_i e^{-a_i t} \xrightarrow{L} \sum_{i=1}^4 \frac{A_i}{(s + a_i)} \quad (1)$$

This empirical formula was then equated to a theoretical transfer function, $V(s)$, that includes a zero in addition to the four poles (adapted from Ref. [22]):

$$V(s) = \frac{K(s + z)a_1 a_2 a_3 a_4}{(s + a_1)(s + a_2)(s + a_3)(s + a_4)} \quad (2)$$

Through application of Heaviside's method for expansion of partial fractions, the two forms of the transfer function are found to be related by equations of the form:

$$A_1 = \frac{K(z - a_1)a_2 a_3 a_4}{(a_2 - a_1)(a_3 - a_1)(a_4 - a_1)} \quad (3)$$

Nonlinear regression produced the values of the exponential rate constants and amplitude coefficients reported

in the Results section as well as the rate constant for the zero, $z = 2.02 \pm 2.03 \text{ s}^{-1}$, which is close to the predicted value of 0; K is an arbitrary scaling factor in this context.

Current-source density (CSD) analysis involves the calculation of the second derivative of the field potential with respect to position [32]. These calculations were made for the dimension perpendicular to the cortical surface, with the implicit assumption that only negligible amounts of current flowed in the other dimensions. Furthermore, the actual conductivity was not measured, so a uniform value of unity was assumed. The approximate CSD was calculated according to this formula:

$$\frac{\partial^2 \Phi}{\partial z^2} \approx \frac{\Phi(z + n \Delta z) - 2\Phi(z) + \Phi(z - n \Delta z)}{(n \Delta z)^2} \quad (4)$$

The field potential (Φ), recorded with the silicon probe, is a function of position (z), with $\Delta z = 100 \mu\text{m}$. The CSD calculation may be made with nearest neighbor points ($n = 1$), next nearest neighbors ($n = 2$), and so on. Calculating the CSD with more distant points has the effect of smoothing the data and results in a loss of spatial resolution [35]. Furthermore, $2n$ data points are lost at each end of the array. Interestingly, to calculate the CSD with $n = 2$ is mathematically equivalent to first smoothing the data according to Eq. 5 with $a = 2$ and $b = 1$, then calculating the CSD with $n = 1$:

$$\Phi_{\text{smoothed}} = \frac{b\Phi(z + \Delta z) + a\Phi(z) + b\Phi(z - \Delta z)}{c}, \quad (5)$$

where $c = a + 2b$.

Field potential data were smoothed as above and the CSD was calculated with nearest neighbor points, with two additional modifications. Endpoints were averaged with penultimate points, with a 2:1 weighting. This allowed a CSD estimate to be made for the penultimate points. The other modification was based on the assumption that the field potential generator could be approximated by a planar dipole field. Under this assumption, the decrement in local field potential (LFP) amplitude a small distance from the cortex (100 μm), in a conductive bath, would be small. Therefore, by creating a fictive channel 100 μm from the cortical surface, with the same potential as the surface channel, it was possible to estimate the CSD at the surface.

3. Results

3.1. Oscillatory evoked potentials (EP) from awake and anesthetized rats

The local field potential (LFP) is generated by the summed extracellular currents representing the net activity of all neurons in the EC and is significantly correlated to the firing of individual neurons within the cortex [9,12,14].

Whereas the firing of a single neuron may have no profound effect by itself, the massive coordination of neurons implied by a macroscopically observable field potential is likely to powerfully influence the recipient neural populations. Thus, the LFP provides a readout of the dominant temporally and spatially correlated modes of activity within a cortical region.

In order to study the dynamics of olfactory driven activity in the EC, we recorded the LFP resulting from brief (0.01 ms) biphasic electrical impulses applied to the LOT. The compound action potential thus generated arrives at the apical dendrites of the principal cells of the EC (stellate and pyramidal cells in layers II and III, respectively), where excitatory postsynaptic currents (EPSCs) flow, resulting in the first surface-negative peak of the evoked potential. Our recordings in awake and lightly anesthetized animals were similar in that there were multiple zero crossings and the responses decayed to baseline over ~ 100 ms (Fig. 1). All subsequent results were derived from experiments in anesthetized animals.

The amplitude of the first negative peak varied in proportion to the stimulus current applied, although the slope of this relationship varied, depending upon the efficacy of the stimulation site. The latency to the first peak was between 6 and 12 ms, depending upon the recording location, while the rise time was constant. Fig. 2 shows a series of responses to increasing stimulus intensities, illustrating the linear relationship between the stimulus and first peak and the nonlinearity of subsequent peaks. As the stimulus amplitude increased, the latency of all peaks after the first increased, while their amplitudes grew in a

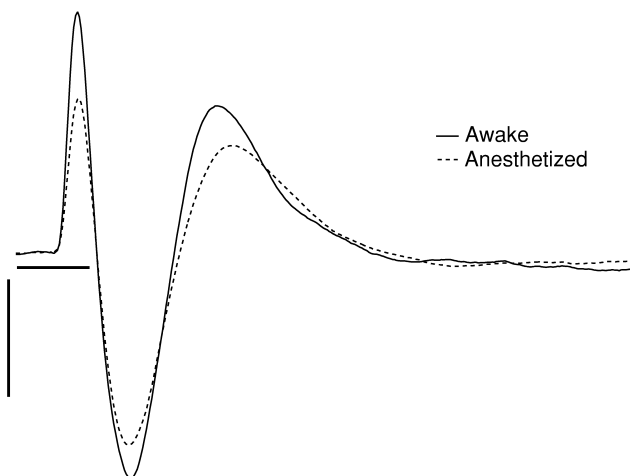


Fig. 1. Evoked potentials in awake and lightly anesthetized rats. The initial negative peak (shown upward, a convention used throughout this paper) represents a negative potential at the cortical surface resulting from current flowing into the apical dendrites that receive synaptic input from the lateral olfactory tract (LOT). Subsequent peaks indicate propagation of activity and feedback within the cortical circuit. Stimulus pulses of 0.01-ms duration were applied to the LOT at time 0. Time scale bar represents 20 ms and amplitude scale bar represents 20 μ V.

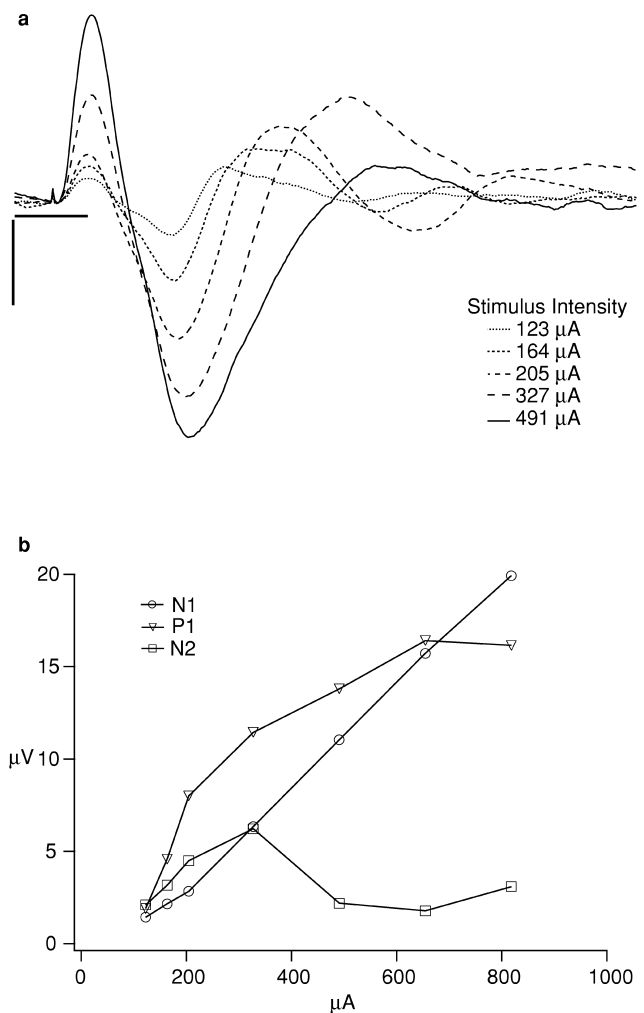


Fig. 2. Responses to increasing stimulus amplitudes. Part (a) shows a series of evoked potentials resulting from increasing stimulus currents. Only low amplitude stimulus/response pairs are shown, for clarity. Time scale bar represents 20 ms and amplitude scale bar represents 5 μ V. Part (b) depicts the absolute value of peak amplitude versus stimulus current for first (N1), second (P1), and third peaks (N2). P1 and N2 show diminishing growth for higher amplitude stimulation owing in part to output clipping (see text).

sublinear manner (Fig. 2a,b). This form of nonlinearity has been observed in the olfactory cortex [4] and is explained by a negative feedback model in which strong activation of inhibitory neurons reduces the activity of the excitatory neurons below their individual thresholds, clipping the population response, and reducing the subsequent peaks of the damped oscillatory response.

The similarity in form of these responses to those observed in prepiriform cortex (PPC, or olfactory cortex) following LOT stimulation [16,18,19,29], as well as the structural resemblance between PPC and the superficial three layers of EC, led us to attempt an open loop circuit analysis, i.e. a study in which the paths of neural feedback within the cortex are pharmacologically or surgically nullified [22], with the goal of identifying the components

of the cortical circuit that shape the EC's response to olfactory input.

3.2. Open loop EPs from deeply anesthetized animals

As the animal falls more deeply under the influence of anesthesia, the typical evoked response becomes less oscillatory until, in the extreme, it is nearly monophasic (Fig. 3). We hypothesized that the excitatory and inhibitory neurons within the cortex are normally in a quasi-steady state, with each population having a characteristic basal firing rate. This activity is dependent upon an excitatory drive that sustains the EC in a responsive state, such that

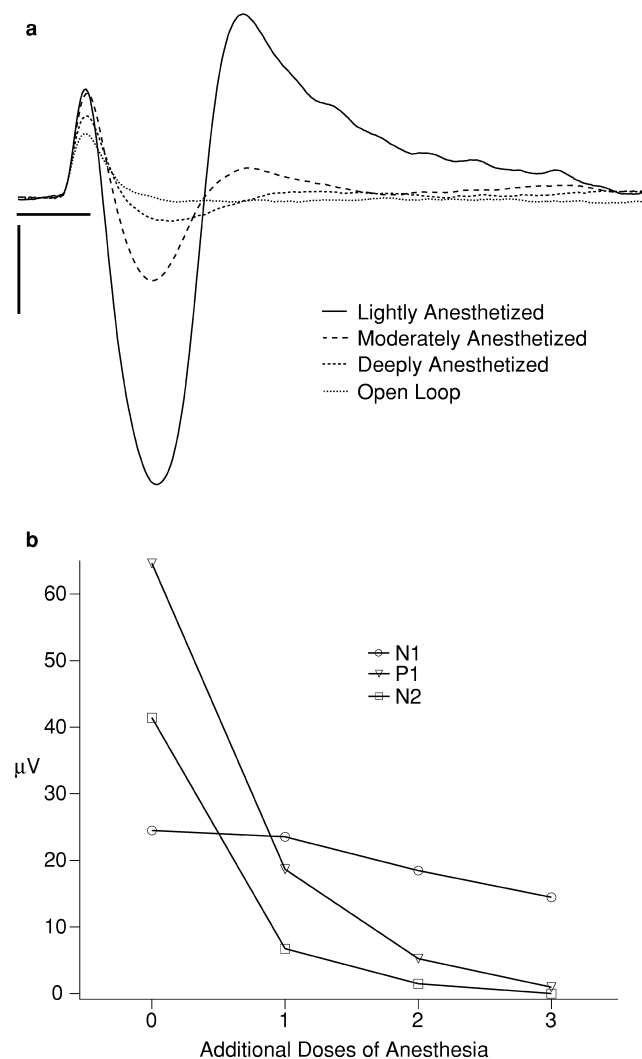


Fig. 3. Progression toward the open loop state. Part (a) shows evoked potentials from one animal under successively greater doses of anesthesia. Responses show a disproportionate reduction in the amplitude of later peaks, until the non-oscillatory open loop state is reached. Time scale bar represents 20 ms and amplitude scale bar represents 20 μV . In part (b) a graph of the magnitudes of the first and second negative peaks and the first positive peak further illustrate the damping effect of anesthesia on oscillatory activity.

slight perturbations can propagate through the system, producing recurrent excitation and inhibition, and resulting in the oscillations observed in evoked potentials. We concluded, therefore, that by reducing total brain activity with a barbiturate anesthetic we had removed a pervasive excitatory bias, essentially turning off the EC.

The non-oscillatory responses produced under deep anesthesia display essentially the same latency, rise time, and linear dependence of amplitude on stimulus intensity as the initial response peaks from awake and lightly anesthetized animals. However, the surface-negative (N1) potentials do not end abruptly at zero but decay exponentially back to baseline with a characteristic time constant followed by a prolonged low-amplitude surface positive potential. We interpret the main peak as resulting from stimulated EPSCs in the apical dendrites of the principal cells, with the slower decay rate representing the termination of synaptic currents, unobscured by the polysynaptic potentials and recurrent activity produced in the closed loop state. The surface-positive overshoot may be due to the homeostatic reflux of ions in the dendrites following the cessation of synaptic activation [22].

We quantified these responses by fitting the averaged evoked potentials from each animal with a transfer function expressed as the sum of four exponential terms — four being the optimal number for robust convergence using a nonlinear regression algorithm, in this case:

$$\sum_{i=1}^4 A_i e^{-a_i t} = -7.78e^{-78.1t} + 27.3e^{-154t} - 23.4e^{-289t} + 3.97e^{-802t} \quad (6)$$

Eq. 6 shows the computed formula for the open loop evoked potential and Table 2 shows the rate constants with their estimated standard errors. The curve fitting procedure was able to account for greater than 95% of the variability in all 'open loop' evoked potentials. The form of responses under deep anesthesia is similar to those reported in PPC and OB; however, the dominant decay time constant ($1/a_1$, or 6.48 ms) is greater than the corresponding decay times found in those structures in cats (4.48 ± 0.36 ms for PPC, following LOT stimulation [17], 4.42 ± 0.22 ms for OB, following LOT stimulation and 4.74 ± 0.18 ms following primary olfactory nerve stimulation [20]).

Table 2
Exponential rate constants

Rate constant	Average value \pm S.E. (s^{-1})
a_1	78.1 ± 4.12
a_2	154 ± 6.03
a_3	289 ± 10.7
a_4	802 ± 77.9

The open loop response was modeled as the sum of four exponential terms, which are shown here with their estimated standard errors. The corresponding amplitude coefficients may be found in Eq. 6.

These time-domain results are an indication of the total response of the EC circuitry to LOT stimulation. However, the heterogeneous cell populations distributed across the cortical layers are likely to participate in different ways as afferent signals are transmitted through the EC. Our next experiment was aimed at describing the spatial distribution of synaptic currents contributing to the oscillatory and non-oscillatory evoked potentials.

3.3. Current-source density in closed loop and open loop animals

The first surface-negative potential in both the oscillatory (closed loop) and non-oscillatory (open loop) evoked potentials is generated by synaptic currents associated with the input pathway from olfactory bulb, the LOT, which terminates widely in layer 1a [39]. However, when polysynaptic transmission occurs within the EC, the evoked activity is carried to all cell layers. Bipolar recordings provide information about the net field potential across the layers spanned by the electrode pair, but a multielectrode array allows greater spatial resolution of the local neural activity. In this experiment we employed a linear array of electrodes to record the LFP, from which the contribution of neurons in each layer is differentiated by computation of the current-source density, a measure of the current flowing into or out of the cells in the vicinity of the electrode.

The spatiotemporal pattern of neural activity following LOT stimulation is illustrated in Fig. 4. At the minimum level of anesthesia (Fig. 4a), the migration of activity to deeper layers at greater latencies suggests a cascade of polysynaptic activation. The alternations from dark to light and light to dark at a given depth signify changes in the CSD relative to some undetermined baseline level because the original field potential recordings were high pass filtered (see Ref. [6] for a discussion of filtered CSD signals). The repetition of relative sinks and sources at a particular depth indicates recurrent activation of the local synapses, separated by a transient reduction in input, and is taken as evidence for feedback within the neural circuit.

As greater quantities of Nembutal are administered the spatial extent of activation decreases (Fig. 4b). In addition, the timecourse of sink/source alternation within those layers still showing activity is slowed somewhat. At the deepest levels of anesthesia (Fig. 4c,d), polysynaptic activity appears to be curtailed, with no significant transmission to deeper layers and no continued oscillation in the time domain. We interpret this as the open loop state, in which the evoked response is confined to the input layer.

The open loop responses are consistent with the hypothesis that a continual excitatory bias emanating from other brain areas facilitates polysynaptic transmission. However, this might also result from a purely local reaction to the anesthetic. Our next experiments were designed to reduce the excitatory bias reaching the EC, by non-pharmaco-

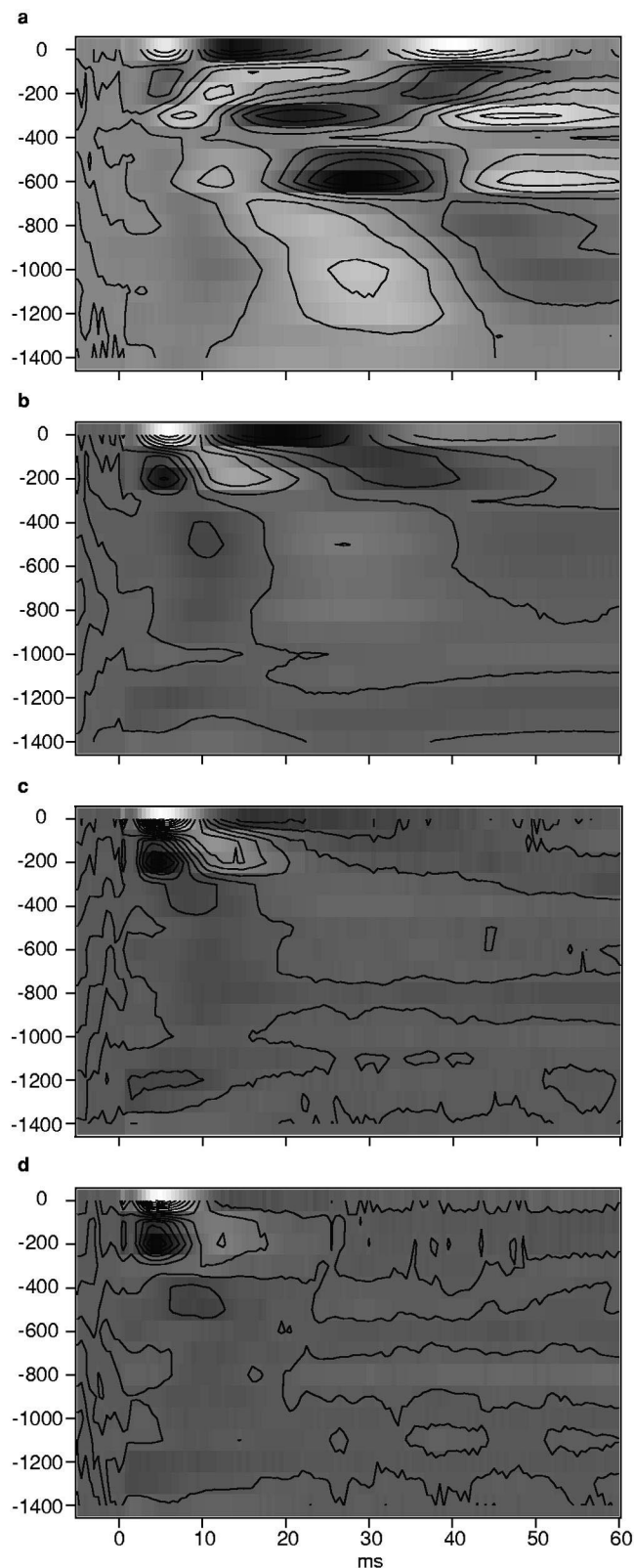


Fig. 4. Current-source density analysis of transition from closed loop to open loop state. Current sinks (plotted in lighter shades) correspond to positive charges entering neurons, as would happen in an EPSC. Sources (plotted in darker shades) result from the return current that must flow out of the neurons in order to balance the movement of charges throughout the tissue. Panels (a)–(d) show the distribution of sources and sinks that generated the time series shown in Fig. 3. Depth in μm .

logical means, in order to observe the dependence of oscillatory responses upon a sustaining excitatory input.

3.4. EPs in bulbotomized animals indicate open loop state

As a test of the idea that there is a net excitatory drive that sustains the EC in a responsive state, we severed one of the greatest single sources of input to the EC, the olfactory bulb [21]. In different experiments this manipulation was achieved by transecting the stalk of the OB, aspirating a portion of the OB stalk, or injecting ~ 0.01 ml lidocaine (2% solution) into the anterior LOT. All three methods immediately suppressed the oscillatory component of the evoked potentials, producing unimodal responses identical to those observed under the deepest general anesthesia (Fig. 3), although the effects of lidocaine injection were transient, wearing off within 20 min.

Fig. 5 shows the average evoked response following bulbotomy compared with the average evoked response under deep anesthesia, with the shaded region indicating ± 1 S.D. from the anesthetized mean (the standard deviation of responses following bulbotomy were < 2 times greater). Furthermore, the open loop evoked potentials following bulbotomy display essentially the same latency, rise time, and linear dependence of amplitude on stimulus intensity as the initial response peaks from intact awake and lightly anesthetized animals. An example of the open loop evoked CSD pattern following bulbotomy is shown in Fig. 6, demonstrating the same superficial sink and source pair as observed in the deeply anesthetized case.

Our final experiment was designed to test whether this non-specific excitatory drive is not only necessary but sufficient to turn on the feedback circuitry in the EC, i.e.

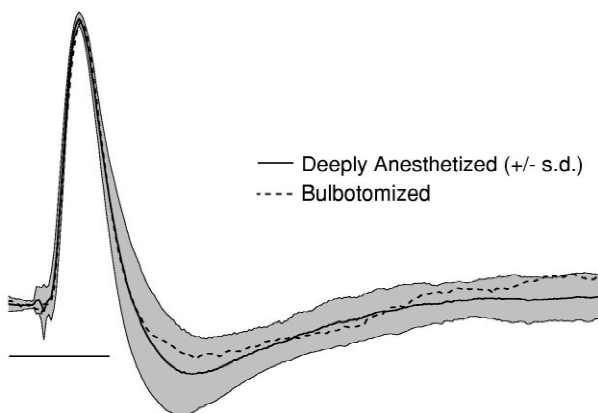


Fig. 5. Average open loop responses. The solid curve represents the average evoked response across all rats in the deeply anesthetized, open loop state. This curve is bounded by one standard deviation (gray shading), indicating the variability of the open loop responses across animals. The dashed curve represents the average evoked response across all bulbotomized rats. Averages were calculated from normalized responses; time scale bar represents 20 ms.

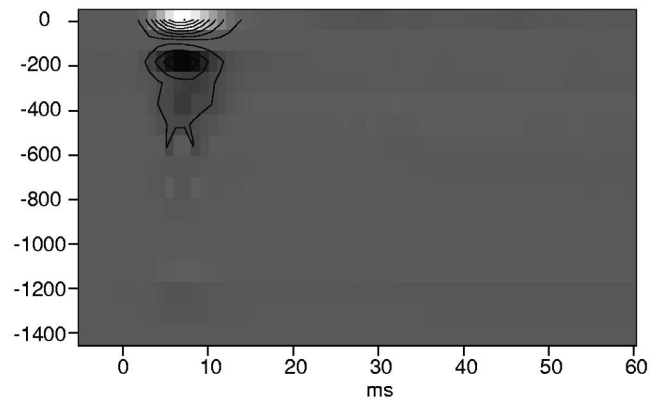


Fig. 6. Current-source density analysis of open loop evoked potential following bulbotomy. The prominent current sink at the cortical surface represents the excitatory postsynaptic currents elicited by the arrival of the compound action potential stimulated in the LOT and is balanced by a source distributed across ~ 300 μm of tissue underlying the sink. Sinks are plotted in lighter shades and sources plotted in darker shades. Depth in μm .

close the loop, thereby re-establishing the oscillatory response.

3.5. Reversal of open loop state by tetanization

It is possible to reinstate the oscillatory character of evoked responses in the bulbotomized EC by providing a substitute excitatory bias. After transecting the LOT (or pharmacologically blocking transmission), we applied a high frequency (200 Hz) activating pulse train to the LOT posterior to the site of transection. At a nearby location along the LOT we applied test pulses while measuring the evoked response in the EC. As the intensity of the activating pulse train was increased, the EPs changed from non-oscillatory, open loop responses to damped oscillations similar to closed loop responses (Fig. 7). With the highest intensity pulse trains, the structure of the EPs became less oscillatory again. Fig. 8 shows two examples of restored oscillations displayed with comparison traces from the same lightly anesthetized animal, prior to bulbotomy, demonstrating that, while similar, the restored oscillatory evoked potentials have a broader initial peak. This broadening of the first peak is interpreted as an effect of bulbotomy, insofar as the inhibition of OB output that normally occurs by virtue of the antidromic volley induced by electrical stimulation of the LOT that excites the granule cells causing them to inhibit the mitral cells' background activity no longer exists and is therefore incapable of influencing the EC [38].

The application of a high frequency pulse train to the LOT does not produce a permanent change in the open loop evoked potential. Fig. 9 shows the open loop response before and after application of the pulse train. Fig. 9 also shows that the response produced by an identical test pulse, in the presence of a 3.27-mA, 200-Hz pulse train,

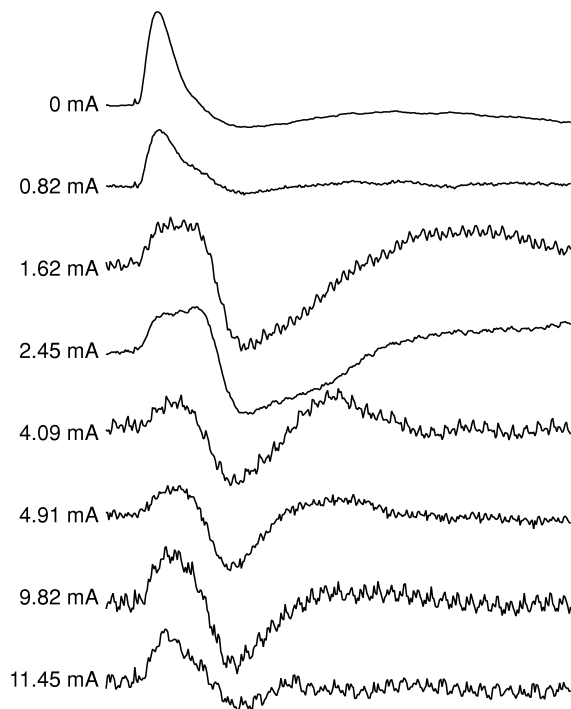


Fig. 7. Reversal of open loop by application of pulse train. Average evoked potentials elicited by 0.82-mA, 0.01-ms test pulses applied to the LOT, subsequent to bulbotomy. The top trace is the open loop response resulting from the loss of bulbar activation. Subsequent traces were recorded during the application of a 200-Hz pulse train to a secondary LOT site, providing tonic excitatory input to the EC and enabling oscillatory responses. Pulse train amplitudes are indicated next to the traces; amplitude scale bar represents 10 μ V and time scale bar represents 20 ms.

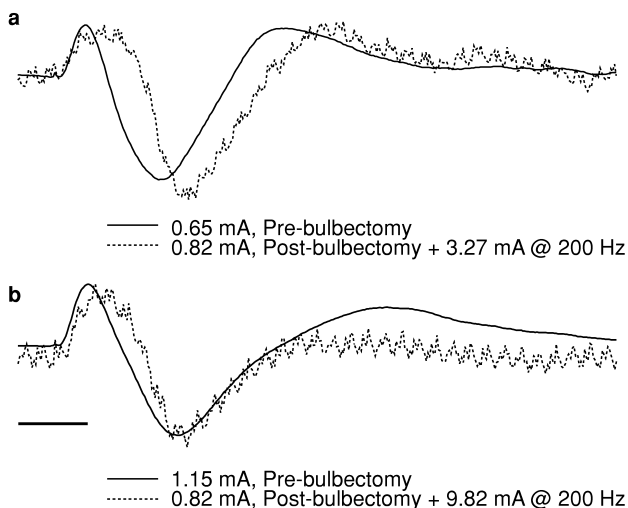


Fig. 8. Comparison of waveforms in whole and bulbotomized rats. Part (a) shows similar responses to a 0.65-mA test pulse in an intact animal and a 0.82-mA test pulse in a bulbotomized animal, which was receiving a 3.27-mA, 200-Hz pulse train at a different LOT site. Part (b) compares responses to a 1.15-mA test pulse in an intact animal and a 0.82-mA test pulse in a bulbotomized animal, which was also receiving a 9.82-mA, 200-Hz pulse train. Amplitudes are normalized to first negative peak for comparison of shape; time scale bar represents 20 ms.

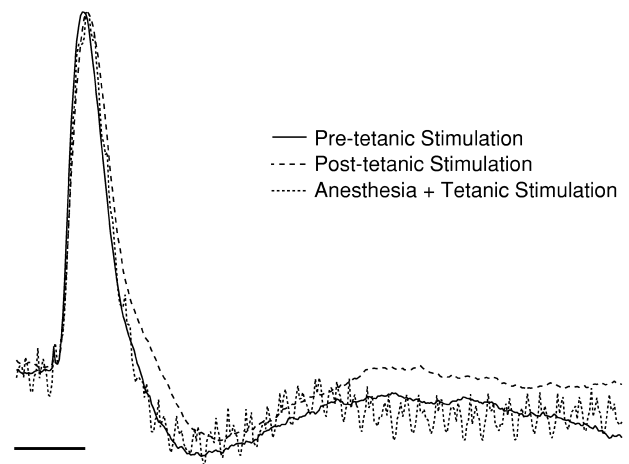


Fig. 9. Open loop EPs resulting from 0.82-mA test pulses. The solid and dashed traces were obtained before and after high frequency stimulation, respectively. The dotted trace was obtained with a 3.27-mA, 200-Hz pulse train after a large dose of pentobarbital, showing the combined effect of surgical and pharmacological activity blockade in reducing cortical responsiveness. Amplitudes are normalized and time scale bar represents 20 ms.

shortly after administration of a dose of Nembutal is open loop. The inability to evoke an oscillatory response in this case implies that surgical and pharmacological blockade of excitatory input to the EC act synergistically, reducing cortical excitability to such an extent that the pulse train is ineffective at reactivating the cortex. Alternatively, the anesthesia may be acting locally within the EC, making the cortical feedback circuit refractory to all stimuli.

4. Discussion

Our results show that electrical pulse stimulation of the LOT produces characteristically oscillatory responses in the EC that are mediated by polysynaptic (feedback and feedforward) transmission through the cortical layers. The efficacy of transmission and the form of the oscillatory response depend upon the background level of activity impinging on the EC from elsewhere in the brain. Pharmacological and surgical manipulations blocked this ambient excitatory bias and so eliminated polysynaptic transmission and oscillations. The EC was restored to a state capable of supporting oscillatory responses by applying a high frequency pulse train to a parallel input pathway, thereby supplying a substitute source of background excitation.

The relationship between neuronal firing probability and the local field potential, throughout the olfactory system and entorhinal cortex, has been described by a sigmoid function [13]. The sigmoid relationship reflects the spectrum of nonlinear input–output functions for a neural population, from depressed unresponsiveness through a state of maximal excitability to unresponsive saturation [22,23]. In this theoretical framework the closed loop

responses in EC represent a reverberation of the initial stimulus through a feedback network of excitable cells, i.e. the neural population would be described by the steepest region of the sigmoid curve in Fig. 10a. Barbiturate anesthesia, in the doses used to induce the open loop state, opens GABA_A receptor chloride channels [27], thereby hyperpolarizing most cortical neurons [24,34] and shunting current in any case. This should reduce the effectiveness of synaptic input in producing action potentials and corresponds to a leftward/downward shift along the sigmoid curve. Likewise, removing the incident excitatory drive emanating from the OB allows the entire cortical population to relax to the flat, unresponsive, lower end of the sigmoid function. Finally, replacing the excitatory bias from OB with a high frequency pulse train drives the cortical network upward along the sigmoid, through a responsive range, to the ceiling, where additional stimulation produces no further response in the form of additional action potentials. The reduced growth of P1 and N2 (Fig. 2) with increasing amplitude of N1 is imposed by the thresholds of the excitatory neurons. When these neurons are inhibited to zero firing rates, they cannot respond to further inhibition below their thresholds, and therefore cannot proportionately disexcite the inhibitory neurons in the feedback loop, explaining the sublinear growth of P1 and N2 amplitudes and the broadening of N1 in Fig. 2, as

well as the failure to achieve robust oscillations with the highest amplitude pulse train in Fig. 7.

The olfactory system is behaviorally very important for rats [37]. Here we have shown that its importance extends beyond olfaction per se, in that its mere activity is necessary (and in some sense, sufficient) for the generation of normal responses in another brain area, the entorhinal cortex. If this type of functional dependence upon excitatory input is common throughout the brain, it invites a reinterpretation of ‘disconnection syndromes’. These syndromes result from lesions of fiber pathways in the brain, and are usually interpreted as deficits of information transfer [10]. However, a deficit of activating bias may leave a cortical region unable to respond to input, functionally disconnecting it from the rest of the brain and interrupting the global processing in which it participates. For example, the behavioral result of olfactory bulbotomy in rats is a syndrome that includes crossmodal learning and memory deficits typically associated with limbic system dysfunction, as well as other symptoms of depression [26,28]. This suggests that the excitatory bias produced by olfactory bulb activity sustains normal functions in the limbic system and thereby enables normal behavior in the animal.

Acknowledgements

This research was supported by grant MH06686 from the National Institute of Mental Health. Silicon probes were provided by the University of Michigan Center for Neural Communication Technology (sponsored by NIH/NCRN grant P41 RR09754).

References

- [1] A. Alonso, E. Garcia-Austt, Neuronal sources of theta rhythm in the entorhinal cortex of the rat. I. Laminar distribution of theta field potentials, *Exp. Brain Res.* 67 (1987) 493–501.
- [2] H. Ansel, D.B. Lindsley, Differentiation of two reticulo-hypothalamic systems regulating hippocampal activity, *Electroencephalogr. Clin. Neurophysiol.* 32 (1972) 209–226.
- [3] S.N. Baker, E. Olivier, R.N. Lemon, Coherent oscillations in monkey motor cortex and hand muscle EMG show task-dependent modulation, *J. Physiol. (Cambridge)* 501 (1997) 225–241.
- [4] M. Biedenbach, W. Freeman, Linear domain of potentials from the prepyriform cortex with respect to stimulus parameters, *Exp. Neurol.* 11 (1965) 400–417.
- [5] P.H. Boeijinga, F.H. Lopes da Silva, Differential distribution of beta and theta EEG activity in the entorhinal cortex of the cat, *Brain Res.* 448 (1988) 272–286.
- [6] J. Brankack, M. Stewart, S.E. Fox, Current source density analysis of the hippocampal theta rhythm: associated sustained potentials and candidate synaptic generators, *Brain Res.* 615 (1993) 310–327.
- [7] S.L. Bressler, The gamma wave: a cortical information carrier?, *Trends Neurosci.* 13 (1990) 161–162.
- [8] S.L. Bressler, W.J. Freeman, Frequency analysis of olfactory system

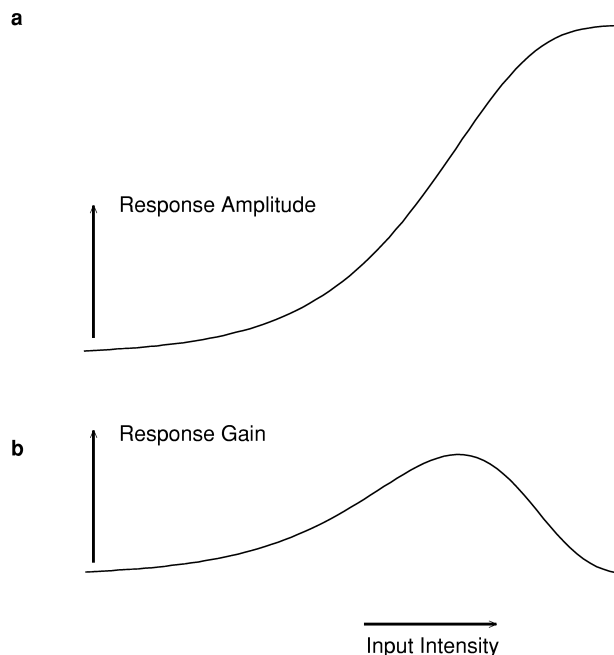


Fig. 10. Asymmetric sigmoid function relating neural population output to input [23]. The horizontal axes in (a) and (b) represent the total level of input to a neural population. The sigmoid function in (a) shows how the population activity increases with input. The slope of the sigmoid function (graphed in b) represents the gain of the population and shows that the incremental increase of activity resulting from a test pulse is maximal at intermediate levels of input, but falls off at low and high levels of input.

- EEG in cat, rabbit, and rat, *Electroencephalogr. Clin. Neurophysiol.* 50 (1980) 19–24.
- [9] J.J. Chrobak, G. Buzsaki, Gamma oscillations in the entorhinal cortex of the freely behaving rat, *J. Neurosci.* 18 (1998) 388–398.
- [10] R.E. Cytowic, *The Neurological Side of Neuropsychiatry*, MIT Press, Cambridge, MA, 1996, pp. 529.
- [11] C.T. Dickson, I.J. Kirk, S.D. Oddie, B.H. Bland, Classification of theta-related cells in the entorhinal cortex: cell discharges are controlled by the ascending brainstem synchronizing pathway in parallel with hippocampal theta-related cells, *Hippocampus* 5 (1995) 306–319.
- [12] F.H. Eckman, W.J. Freeman, Correlations between unit firing and EEG in the rat olfactory system, *Brain Res.* 528 (1990) 238–244.
- [13] F.H. Eckman, W.J. Freeman, Asymmetric sigmoid nonlinearity in the rat olfactory system, *Brain Res.* 557 (1991) 13–21.
- [14] M.S. Fee, P.P. Mitra, D. Kleinfeld, Central versus peripheral determinants of patterned spike activity in rat vibrissa cortex during whisking, *J. Neurophysiol. (Bethesda)* 78 (1997) 1144–1149.
- [15] R. Fettiplace, Electrical tuning of hair cells in the inner ear, *Trends Neurosci.* 10 (1987) 421–425.
- [16] W. Freeman, Repetitive electrical stimulation of prepyriform cortex in cat, *J. Neurophysiol.* 23 (1960) 383–396.
- [17] W.J. Freeman, A linear distributed feedback model for prepyriform cortex, *Exp. Neurol.* 10 (1964) 525–547.
- [18] W.J. Freeman, Patterns of variation in waveform of averaged evoked potentials from prepyriform cortex of cats, *J. Neurophysiol.* 31 (1968) 1–13.
- [19] W.J. Freeman, Linear analysis of the dynamics of neural masses, *Annu. Rev. Biophys. Bioengin.* 1 (1972) 225–256.
- [20] W.J. Freeman, Measurement of open-loop responses to electrical stimulation in olfactory bulb of cat, *J. Neurophysiol.* 35 (1972) 745–761.
- [21] W.J. Freeman, Measurement of oscillatory responses to electrical stimulation in olfactory bulb of cat, *J. Neurophysiol.* 35 (1972) 762–779.
- [22] W.J. Freeman, in: *Mass Action in the Nervous System: Examination of the Neurophysiological Basis of Adaptive Behavior Through the EEG*, Academic Press, New York, 1975, p. xx, 489 pp.
- [23] W.J. Freeman, Nonlinear gain mediating cortical stimulus–response relations, *Biol. Cybern.* 33 (1979) 237–247.
- [24] W.J. Freeman, Valium, histamine, and neural networks, *Biol. Psychiatry* 34 (1993) 1–2.
- [25] C. Hölscher, R. Anwyl, M.J. Rowan, Stimulation on the positive phase of hippocampal theta rhythm induces long-term potentiation that can be depotentiated by stimulation on the negative phase in area CA1 in vivo, *J. Neurosci.* 17 (1997) 6470–6477.
- [26] J.A. Jesberger, J.S. Richardson, Animal models of depression: parallels and correlates to severe depression in humans, *Biol. Psychiatry* 20 (1985) 764–784.
- [27] G.A. Johnston, M. Willow, Barbiturates and GABA receptors, *Adv. Biochem. Psychopharmacol.* 26 (1981) 191–198.
- [28] J.P. Kelly, A.S. Wrynn, B.E. Leonard, The olfactory bulbectomized rat as a model of depression: an update, *Pharmacol. Ther.* 74 (1997) 299–316.
- [29] K.L. Ketchum, L.B. Haberly, Membrane currents evoked by afferent fiber stimulation in rat piriform cortex. I. Current source-density analysis, *J. Neurophysiol.* 69 (1993) 248–260.
- [30] R. Klink, A. Alonso, Ionic mechanisms for the subthreshold oscillations and differential electroresponsiveness of medial entorhinal cortex layer II neurons, *J. Neurophysiol.* 70 (1993) 144–157.
- [31] R. Kramis, C.H. Vanderwolf, B.H. Bland, Two types of hippocampal rhythmical slow activity in both the rabbit and the rat: relations to behavior and effects of atropine, diethyl ether, urethane, and pentobarbital, *Exp. Neurol.* 49 (1975) 58–85.
- [32] U. Mitzdorf, Properties of the evoked potential generators: current source-density analysis of visually evoked potentials in the cat cortex, *Int. J. Neurosci.* 33 (1987) 33–59.
- [33] G. Paxinos, C. Watson, in: *The Rat Brain in Stereotaxic Coordinates*, 2nd Edition, Academic Press, Sydney, 1986, p. xxvi, 237 pp.
- [34] L. Siklos, M. Rickmann, F. Joo, W.J. Freeman, A.J.R. Wolff, Chloride is preferentially accumulated in a subpopulation of dendrites and periglomerular cells of the main olfactory bulb in adult rats, *Neuroscience* 64 (1995) 165–172.
- [35] C.E. Tenke, C.E. Schroeder, J.C. Arezzo, H.G. Vaughan Jr., Interpretation of high-resolution current source density profiles: a simulation of sublaminar contributions to the visual evoked potential, *Exp. Brain Res.* 94 (1993) 183–192.
- [36] R.D. Traub, M.A. Whittington, S.B. Colling, G. Buzsaki, J.G.R. Jefferys, Analysis of gamma rhythms in the rat hippocampus in vitro and in vivo, *J. Physiol. (Cambridge)* 493 (1996) 471–484.
- [37] W.I. Welker, Analysis of sniffing of the albino rat, *Behaviour* 22 (1964) 223–244.
- [38] T.J. Willey, W.J. Freeman, Alteration of prepyriform evoked response following prolonged electrical stimulation, *Am. J. Physiol.* 215 (1968) 1435–1441.
- [39] F.G. Wouterlood, J. Nederlof, Terminations of olfactory afferents on layer II and III neurons in the entorhinal area: degeneration–Golgi–electron microscopic study in the rat, *Neurosci. Lett.* 36 (1983) 105–110.